Catalysis Science & Technology

Accepted Manuscript

ROYAL SOCIETY OF CHEMISTRY

www.rsc.org/catalysis

Journal Name

RSCPublishing

ARTICLE

Isotopic Probes for Ruthenium-Catalyzed Olefin Metathesis

Cite this: DOI: 10.1039/x0xx00000x

Justin A. M. Lummiss, Adrian G. G. Botti, Deryn E. Fogg*

Received 00th January 2012,
Accepted 00th January 2012

DOI: 10.1039/x0xx00000x

www.rsc.org/

Routes are described to previously unreported first- and second-generation Grubbs metathesis catalysts bearing a ^{13}C label at the key benzylidene or methylidene site. Improved syntheses of the ^{2}H-labelled isotopologues are also presented. Labelling at the alkylidene position is important because it provides unique, direct information about changes at the active site of the catalyst, and the fate of the [Ru]=CHR ligand during catalyst deactivation. A case study demonstrates the power of ^{13}C-labelling in tracking the methylidene moiety in amine-induced decomposition of the second-generation complex $RuCl_2(PCy_3)(H_2IMes)(=^{13}CH_2)$. Also reported is the solubility of ethylene in C_6D_6 and CD_2Cl_2, measured at 296 ±1.5K and 101.0 ±0.8kPa.

Introduction

Olefin metathesis is now a core tool in organic synthesis.[1-4] With industrial applications of molecular metathesis catalysts now emerging,[1] improved understanding of their deactivation pathways is becoming increasingly urgent, particularly for the dominant ruthenium catalysts. Isotopic labelling has long been an important tool in organometallic chemistry, enabling direct insight into the rates and fates of bond-forming and bond-breaking reactions via NMR and mass spectrometric (MS) analysis.[5-7] Within the context of olefin metathesis, experiments with labelled olefins afforded key evidence for the Chauvin mechanism,[8-10] for the chain-carrying role of metal alkylidene intermediates,[11] and for the relative competence of ring-closing[12,13] or cross-metathesis[14,15] relative to degenerate exchange. Deuterium-labelled *N*-heterocyclic carbene (NHC) ligands have also been used[16,17] to probe C-H activation during catalyst deactivation and to track the release and return of solid-supported metathesis catalysts.[18]

The present work was motivated by the potential offered by isotopic labelling for insight into the operation and decay[19] of the Grubbs catalysts, which remain among the most important catalyst systems used in olefin metathesis.[1,2] We were particularly interested in accessing derivatives bearing a ^{13}C tag at the key Ru=*C*HR site (Figure 1a). Labelling at the alkylidene position is of keen interest because this reports directly on changes at the active site. The diagnostic potency of the ^{13}C isotope, relative to the more routinely incorporated isotope ^{2}H, is a function of its order-of-magnitude expansion of the NMR chemical shift window, as well as elimination of potential scrambling pathways (a particular issue for catalytically promiscuous metals such as ruthenium). Also significant are the higher receptivity and slower T_2 relaxation relative to deuterium,[20] which significantly improve resolution, while drastically reducing acquisition time.

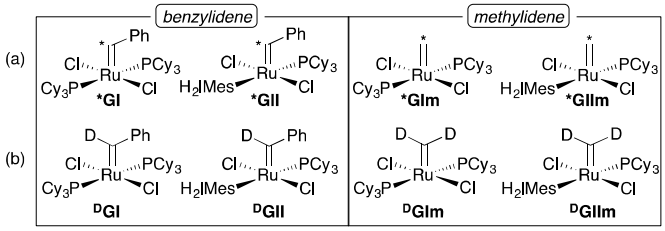

Figure 1. Isotopically labelled targets synthesized in this work. (a) ^{13}C-tagged (*) and (b) ^{2}H-tagged (D) first- and second-generation Grubbs catalysts, and their methylidene resting states. (H_2IMes = N,N′-bis(mesityl)imidazolin-2-ylidene).

Marciniec and co-workers recently reported successful ^{13}C-labelling of the Hoveyda catalyst at the benzylidene carbon, and use of the labelled complex to confirm catalyst anchoring on silica supports.[21] In subsequent studies, this compound was invaluable in affording unequivocal evidence for re-uptake of the styrenyl ether ligand during metathesis.[22] Similarly labelled Fischer carbene complexes earlier revealed transformation of the $[Ru]=^{13}CHOCH_2Ph$ unit into a ruthenium hydridocarbonyl moiety.[23] To date, however, Grubbs catalysts bearing an isotopic label at the alkylidene site are limited to deuterated derivatives.[24-27] Here we report routes to the ^{13}C-labelled analogues, for both first- and second-generation Grubbs catalysts (Figure 1a). In the course of optimizing these syntheses with less costly ^{2}H-labelled reagents, we improved

routes to the known[24-26] deuterated isotopologues **^{D}GI**, **^{D}GIm**, and **^{D}GIIm**, and developed the first route to the deuterated second-generation Grubbs catalyst, **^{D}GII** (Figure 1b).

Results and discussion

First-generation catalysts via labelled styrenes

Cross-metathesis of **GI** with isotopically-labelled styrenes offers a convenient means of installing a *labelled* benzylidene moiety on the first-generation Grubbs catalyst, as demonstrated by Dinger and Mol[25] in synthesis of **^{D}GI**. A challenge, however, lies in the selectivity for the labelled benzylidene complex – that is, the kinetic product – relative to the unwanted thermodynamic product, methylidene **GIm** (Scheme 1). Clean interception of labelled **GI** is especially important because the similar solubilities of these species hampers their separation.

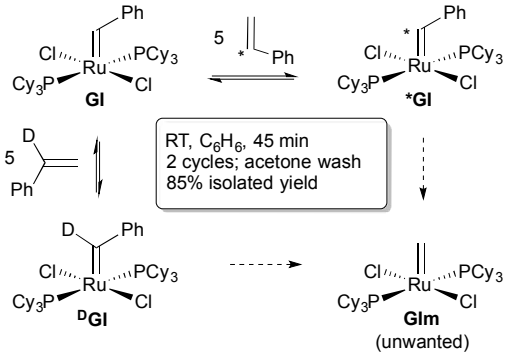

Scheme 1. Kinetic vs. thermodynamic selectivity in synthesis of labelled **GI**.

We find that the timescale for degenerate exchange is much more readily established for ^{13}C-labelled ***GI** than ^{2}H-labelled **^{D}GI**. The doublet multiplicity of the ^{1}H NMR signal for the benzylidene proton in ***GI** (Figure 2: δ_H 20.61 ppm; $^{1}J_{CH}$ = 146.6 Hz) provides a unique, convenient means of simultaneously quantifying both formation of ***GI**, and conversion of **GI**. This is especially useful in conjunction with use of an internal standard to detect net loss of [Ru]=C*H*R species (i.e. decomposition to non-alkylidene products). In the corresponding reactions with H_2C=CDPh, in contrast, the starting material and product cannot be simultaneously observed, and exchange is thus difficult to distinguish from decomposition.

To favour interception of the kinetic benzylidene product, we carried out the exchange reaction at RT (glovebox; ca. 27 °C). We chose benzene in preference to dichloromethane as the reaction medium, given the accelerating effect of aromatic solvents on metathesis.[28] On NMR scale, equilibration of **GI** with a five-fold excess of styrene-α-^{13}C was complete within 45 min at RT. Neither **GIm** nor decomposition was evident over 3 h (Figure 2), and the proportion of ***GI** present at equilibrium was 83%, as expected from the 1:5 stoichiometry of unlabelled vs. labelled styrene. Reactions on preparative scale (200 mg **GI**) involved two 45-minute cycles of reaction with styrene-α-^{13}C. After each pass, the solvent was stripped off in the glovebox, and the styrene was extracted with acetone. This treatment gave clean, straightforward access to the previously unreported ^{13}C-labelled ***GI** in 85% yield, with an isotopic purity of 97%.

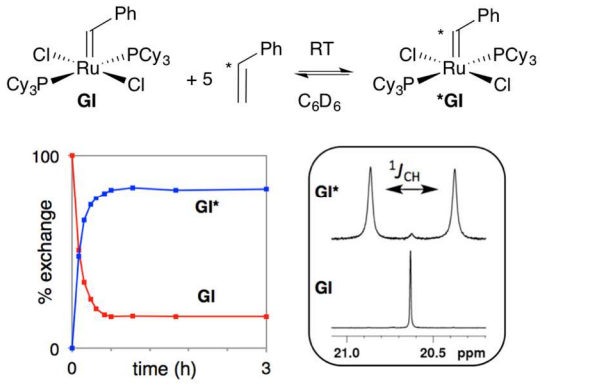

Figure 2. Formation and stability of ***GI** via the method of Scheme 1 (first pass). Inset: Benzylidene region of the ^{1}H NMR spectrum for isolated ***GI** (300 MHz, C_6D_6), illustrating the ease with which crossover can be measured. Lower trace: commercial starting **GI**. Upper trace: ***GI** with 2.2% residual **GI**.

Essentially identical yields and enrichment were obtained in the corresponding synthesis of **^{D}GI** via cross-metathesis of **GI** with styrene-α-D (400 mg scale). Dinger and Mol previously prepared this complex in 62% yield and 95% isotopic enrichment, via a similar sequence involving reaction with 2 x 10 equiv styrene in CH_2Cl_2.[25,29] A key contributor to the nearly 25% increase in isolated yield in the present work (despite the lower proportion of the styrene reagent) is the improved workup procedure. Use of acetone to extract residual styrene, rather than pentane, takes advantage of the sparing solubility of **GI** in acetone.[30] The level of enrichment attainable for these benzylidene targets is limited by (1) the isotopic purity of the styrene reagent; (2) the stoichiometry of the reaction: that is, the equilibrium ratio of unlabelled vs. labelled styrene; and (3) the number of reaction cycles, coupled with the efficiency with which the non-labelled styrene can be extracted.

Labelled second-generation catalysts via ligand exchange

In sharp contrast, synthesis of the labelled second-generation benzylidenes via cross-metathesis of **GII** is unsatisfactory in both yield and purity. The non-lability of the phosphine ligand in **GII** renders exchange very slow (days) at RT, but efforts to accelerate reaction by heating result in co-formation of **GIIm**. As with the first-generation complexes, the benzylidene and methylidene complexes exhibit very similar solubilities, and are not readily separated.

More attractive as an entry point is therefore ligand exchange of labelled **GI** with free H_2IMes (Scheme 2). We previously described the efficiency of this route to **GII**, especially where combined with use of an ion-exchange resin to remove the phosphine co-product and excess NHC.[31] Accordingly, treating ***GI** and **^{D}GI** with free H_2IMes for 1 h in THF at RT, then stirring with Amberlyst resin, enabled access to clean ***GII** and **^{D}GII** in nearly 90% isolated yield (97%

isotopic purity for ***GII**; 96% for **^{D}GII**). It should be noted, however, that the THF must be scrupulously dry to prevent hydrolysis of the free H_2IMes, which adversely affects the reaction stoichiometry, compromising product yields and/or purity.

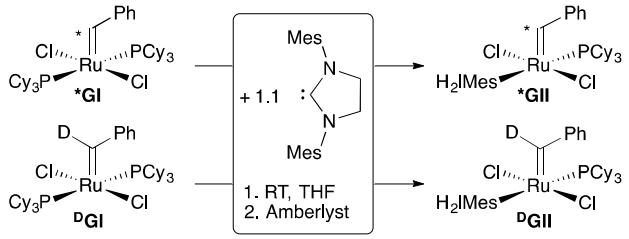

Scheme 2. Successful ligand-exchange route to labelled second-generation benzylidene complexes.

Methylidene complexes: Additional challenges

Synthesis of the labelled methylidene complexes is much more demanding, owing to the instability of these species. A half-life of 6 h has been reported[32] for **GIIm** at 55 °C in C_6D_6, and this figure drops to just 40 min for **GIm**.[33] (For added data concerning the lifetimes of these species, see below). The first-generation methylidene complex **GIm** is nevertheless accessible in high yields and high purity via ethenolysis at RT.[34,35] An alternative route utilizing reaction of $RuH_2(N_2)_2(PCy_3)_2$ with CH_2Cl_2 or CD_2Cl_2 is attractive for circumventing the need for a gaseous labelled reagent.[26] In situ yields of **GIm** or **^{D}GIm** were limited to ca. 65%, however, and the product was contaminated with a $RuHCl(H_2)(PCy_3)_2$ by-product. Also examined in the present study was a potential route involving cross-metathesis with β-labelled styrenes. As this also proved less satisfactory (resulting in <60% ***GIIm**, as a mixture with **GII**), it is briefly described in a closing section.

Our principal focus in this section is on adapting the successful ethenolysis route to permit efficient use of labelled ethylene gas. Sparging to maintain high ethylene concentrations is economically prohibitive, given the high prices of these reagents ($550 or $1400 CAD, respectively, for 1 L of C_2D_4 or $^{13}C_2H_4$ gas; Sigma-Aldrich). Instead, we carried out reactions in sealed vessels, and optimized procedures with deuterated ethylene, before proceeding to the more expensive ^{13}C-labelled gas. As a first step, however, we measured the solubility of dissolved ethylene (a critical parameter in these sealed-tube experiments) in the proposed reaction solvents, using non-labelled ethylene.

Impact of solvent on ethylene solubility and methylidene lifetime

The published data for the solubility of ethylene vary widely. The IUPAC-NIST Solubility Database cites no study as authoritative, although it excludes several values on the basis of unreliability.[36] Given the scatter in the data reported, we measured the solubility of ethylene in CD_2Cl_2 and C_6D_6, at 23 ±1.5 °C. In these experiments, we integrated the ^{1}H NMR singlet for dissolved C_2H_4 against that for a known concentration of trimethoxybenzene (TMB; Figure 3), after saturating the solution in ethylene by five sequential freeze-pump-thaw cycles. An equilibrium concentration of 89 mM was found in C_6D_6, nearly double that in CD_2Cl_2 (54 mM), for experiments in triplicate, using independently-prepared stock solutions.[36]

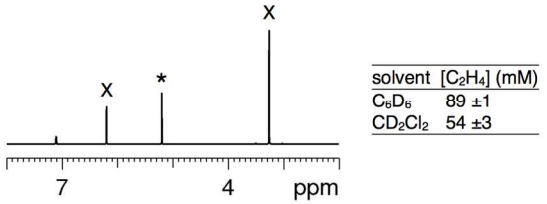

Figure 3. Measuring the solubility of ethylene in organic solvents by ^{1}H NMR analysis (300.1 MHz). Left: representative spectrum. Signal labelled (*) is due to C_2H_4, (×) denotes TMB; C_6HD_5 signal not labelled. Right: tabulated data. Conditions: 296 ±1.5 K, 101.0 ±0.8 kPa, 5 x freeze-pump-thaw cycles prior to equilibrating under ethylene; experiments in triplicate.

Notably, we also find that the highly sensitive methylidene complex **GIm** is much longer-lived in benzene. These experiments were likewise carried out by integrating the signal of interest (in this case, the methylidene singlet) against that for TMB. The half-life in CD_2Cl_2 or $CDCl_3$ was ca. 2.4 h at 35 °C, as compared to 6.6 h in C_6D_6 (Figure 4). Unexpectedly, THF is even more deleterious, with the half-life in this solvent dropping to ca. 1 h. On the basis of both ethylene solubility and product stability, therefore, benzene is preferred for the synthesis of **GIm**.

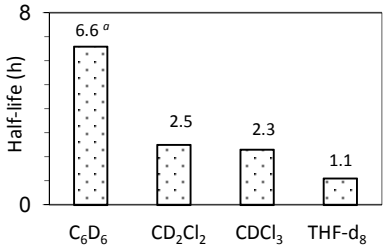

Figure 4. Impact of solvent on the lifetime of **GIm** (18 mM) at 35 °C. Assessed by ^{1}H NMR analysis; integration against TMB as internal standard. [a] Cf. reported half-life at 55 °C in C_6D_6: 40 min.[33]

First-generation methylidenes via labelled ethylene

Following these probe experiments, synthesis of **^{D}GIm** was undertaken on preparative scale (400 mg **GI**). For details of practical measures aimed at maximizing the efficiency of gas delivery from the lecture bottles, readers are referred to the supporting information. Cross-metathesis with C_2D_4 in benzene was conducted in two 45-minute cycles; Scheme 3. After each pass, the solvent was stripped off on the Schlenk line, and the styrene byproduct was extracted with pentane. (Pentane was used in preference to acetone because **GIm** – unlike **GI** – is very sparingly soluble in pentane: this is convenient as pentane residues are more readily removed under vacuum). The first cycle of treatment afforded **^{D}GIm** in 85% isolated yield, with 5% **GI** remaining. A second treatment enabled isolation of

^{D}GIm in 75% total yield (>99% enrichment; no **GI** detected). The corresponding reaction with $^{13}C_2H_4$ afforded ***GIm** in 71% yield (99.5% enrichment). These isolated yields are well below the 85% level that we were able to attain for non-labelled **GIm**.[34] The difference is due in part to the smaller scale for the labelling reactions (400 mg, vs. 1 g). Parallel experiments with C_2H_4 in sealed systems, however, also indicate consistently lower yields relative to the continuously-sparged reactions.

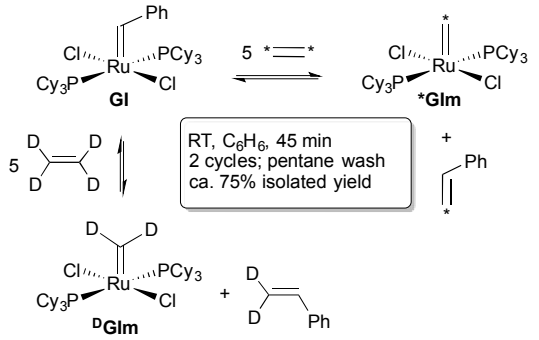

Scheme 3. Synthesis of ***GIm** and **^{D}GIm** by ethenolysis.

Second-generation methylidenes via ligand exchange

Ethenolysis is impractical as a route to the second-generation methylidene complexes. Competing decomposition has been shown to limit isolated yields to 27-36% for **GIIm** or its D-labelled isotopologue.[24,37] More efficient is the "free-carbene" route developed by our group,[34] in which **GIm** is treated with H_2IMes at 60 °C (cf. the corresponding synthesis of the benzylidene complex **GII** described above). The challenge in using this methodology to prepare the methylidene complexes lies in their thermal instability (see Figure 4 and discussion above). Nevertheless, **^{D}GIIm** could be obtained by heating **^{D}GIm** with free H_2IMes for 45 min (Scheme 4). Traces of the decomposition byproduct [$MePCy_3$]Cl were extracted with degassed water (a technique used successfully to refine workup for the non-labelled target, which was obtained in 80% yield for reactions on 700 mg scale; see SI). Free PCy_3 and decomposed Ru were removed by successive extraction with acetone and cold pentane. The partial solubility of the product in these wash solvents limited isolated yields to 60% for reactions on ca. 200 mg scale: the >99% enrichment of the precursor was maintained. Purification with Amberlyst in THF was not feasible for these methylidene complexes, in contrast to the benzylidene analogues discussed above, owing to extensive decomposition.

Use of the same procedure, but omitting the acetone wash, enabled isolation of ***GIIm** in 68% yield (160 mg scale), without any deleterious effect on purity.

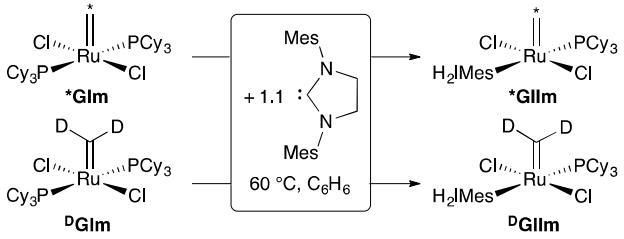

Scheme 4. Synthesis of ***GIIm** and **^{D}GIIm** by ligand exchange.

Limitations in ethylene-free access to labelled methylidenes

Given the cost and technical demands involved in handling the labelled gases, we also explored the potential accessibility of the labelled methylidenes by cross-metathesis with styrene-β-^{13}C (Scheme 5). Here we hoped to exploit the thermodynamic preference for the methylidene species in metathesis of terminal olefins; see above. This approach failed for the synthesis of **GIm**, however. Exchange of **GI** with 5 equiv of styrene at RT was far too slow: NMR-scale reactions proceeded to only 13% **GIm** after 7 days, with 27% net loss of alkylidene (as judged by integration against internal standard). Increasing the temperature to 40 °C caused catalyst degradation to dominate over the desired metathesis exchange: after 28 h at 40°C, just 4% **GIm** was observed, accompanied by 43% decomposition. The corresponding reaction of **GII** with β-^{13}C labelled styrene at 40 °C resulted in a 60:40 mixture of **GII**:***GIIm** after 24 h. Longer reaction increased conversion of **GII**, but at the cost of competing decomposition of ***GIIm**.

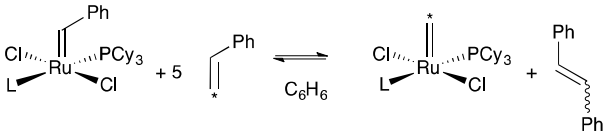

Scheme 5. Potential installation of ^{13}C-labelled methylidenes by cross-metathesis with β-^{13}C-labelled styrene.

Case study: Amine-induced deactivation of GIIm

The ease with which these isotopically labelled complexes enable tracking of the methylidene moiety during catalyst deactivation was tested in a study of the amine-induced decomposition of **GIIm**. Amines have long been regarded as detrimental to ruthenium metathesis catalysts,[38] and have been flagged as problematic in reports from pharma.[1a] We recently demonstrated that during catalysis, sterically accessible primary and secondary amines decompose **GII** via a two-step mechanism, involving (1) replacement of the PCy_3 ligand by amine, and (2) abstraction of the methylidene ligand by the released PCy_3.[39] Given the extreme vulnerability exhibited by **GIIm** during catalysis, however, our original study focused on equimolar proportions of amine relative to catalyst.

Here we wished to examine the susceptibility of the methylidene ligand to *direct* attack by amine. We therefore selected H_2N^nBu, as the least bulky (i.e. most aggressive) of the

amines originally tested, and added it in tenfold excess relative to ***GIIm**. While ^{1}H NMR analysis of non-labelled **GIIm** suffices to reveal loss of the methylidene signal, which is complete within 10 min at RT, the ^{13}C label in ***GIIm** proved invaluable in tracking the fate of the methylidene moiety. Thus, $^{13}C\{^{1}H\}$ NMR analysis at 10 min revealed two dominant species in a ca. 70:30 ratio. These are [*MePCy$_3$]Cl, which appears as a doublet at 1.5 ppm ($^{1}J_{CP}$ = 47.9 Hz), and NH^{n}Bu*Me, a singlet at 36.8 ppm (Figure 5, top).

The ratio of these two species, which reports on the propensity for nucleophilic attack by phosphine, vs. amine, is difficult to ascertain by any other method (including GC analysis, which is hampered by the involatility of the salt). In the absence of the label, $^{13}C\{^{1}H\}$ NMR analysis is of limited use: see inverted spectrum. The signal for the methyl carbon of [*Me*PCy$_3$]Cl (1.52 ppm) is lost in the baseline, and that for NH^{n}Bu*Me* is obscured by H$_2$N^{n}Bu present in excess. The longer acquisition time should also be noted: 5.5 h, vs. 20 min.

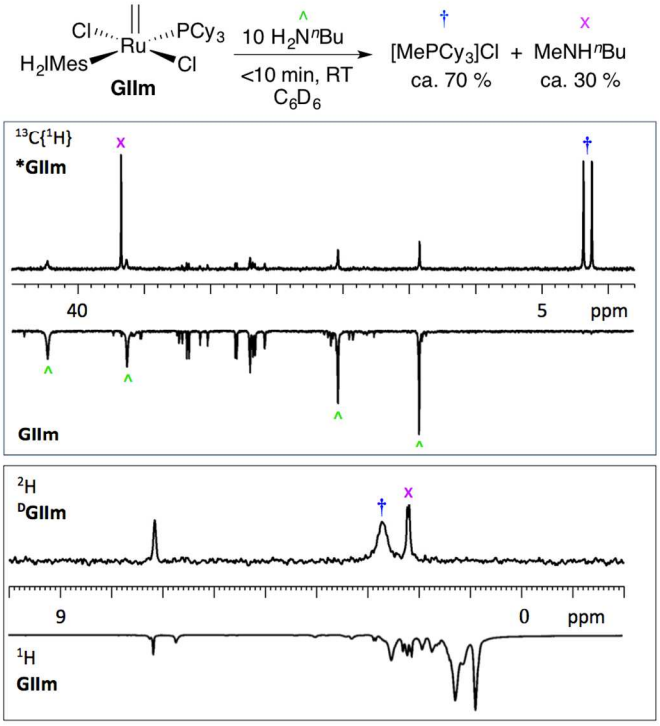

Figure 5. Spectra showing the superior rapidity and clarity with which ^{13}C-labelling enables tracking of the methylidene moiety during decomposition. Top: $^{13}C\{^{1}H\}$ NMR spectra; 20 min acquisition for ***GIIm** and (inverted) 5.5 h acquisition for non-enriched **GIIm**. Bottom: ^{2}H spectrum for ^{D}**GIIm** and (inverted) ^{1}H NMR spectrum for **GIIm** (2 h and 5 min acquisition, respectively).

The corresponding experiment with ^{D}**GIIm** supported the inference from the ***GIIm** experiment, but was less diagnostic. While the methyl signals for [MePCy$_3$]Cl and HN^{n}BuMe can be observed at 2.8 and 2.2 ppm, respectively, assignment is hampered by the poor resolution of the $^{2}J_{DP}$ signal, and the narrow chemical shift window (Figure 5, bottom). It should be noted that neither [MePCy$_3$]Cl nor HN^{n}BuMe can be readily identified by ^{1}H NMR analysis of the non-labelled **GIIm** reaction, as their methyl resonances are obscured by overlapping signals (see inverted spectrum).

These results indicate a surprising bias toward nucleophilic attack by phosphine, relative to amine, even where amine is present in tenfold excess. While the origin of this effect is under further study, the data above illustrate the power of these isotopically labelled complexes, and particularly ^{13}C-labelling at the [Ru]=CHR center, in enabling rapid, quantitative insight into transformations that involve the active site.

Conclusions

The foregoing describes the first synthesis of Grubbs metathesis catalysts bearing a ^{13}C label at the key alkylidene site, as well as improved routes to their ^{2}H-labelled isotopologues. Both first- and second-generation Grubbs catalysts (that is, the benzylidene precatalysts) were prepared, as were their resting-state methylidene complexes. A case study was presented that demonstrates the ease with which the methylidene label can be tracked via the ^{13}C label. This study revealed an unexpected, profound bias for abstraction of the methylidene moiety by phosphine, relative to amine. While the basis for this phenomenon is the subject of ongoing study, the data above illustrate the power of these isotopically labelled complexes for insight into catalyst activation and deactivation, and their potential to expand understanding of the behaviour of the important Grubbs metathesis catalysts.

Experimental

General procedures

Reactions were carried out under N_2 using standard Schlenk and glovebox techniques. Dry, oxygen-free C_6H_6 and CH_2Cl_2 were obtained using a Glass Contour solvent purification system. Pentane was distilled over sodium benzophenone, acetone over calcium sulphate. All solvents were stored under N_2 over Linde 4 Å molecular sieves. C_6D_6 and CD_2Cl_2 (Cambridge Isotopes) were degassed by five successive freeze/pump/thaw cycles and stored over 4Å molecular sieves under N_2 for at least 6 h prior to use. Ethylene (BOC Ultra-High Purity Grade 3.0; 99.9%) was used as received from Linde. The first-generation Grubbs catalyst (**GI**, 97% purity), styrene-α-^{13}C (98% purity, 99% ^{13}C-enrichment, 4-*tert*-butylcatechol as a stabilizer), styrene-α-d_1 (98% purity, 98% ^{2}H-enrichment, hydroquinone as stabilizer), styrene-β-^{13}C (99% ^{13}C-enrichment, 4-*tert*-butylcatechol as stabilizer), $^{13}C_2H_4$ (99% ^{13}C-enrichment), and 1,3,5-trimethoxybenzene (TMB, >99%) were obtained from Sigma-Aldrich, C_2D_4 (99.8% ^{2}H-enrichment) from C/D/N Isotopes. Free H$_2$IMes was prepared by the literature method.[40]

NMR spectra were recorded on a Bruker Avance 300 NMR at 296±1.5 K, and referenced to the residual proton/deuteron or carbon signals of the solvent (^{1}H, ^{2}H, ^{13}C). Signals are reported in ppm, relative to TMS (^{1}H, ^{13}C) or 85% H_3PO_4 (^{31}P) at 0 ppm. The number of intervening bonds for J_{PC} coupling constants is

omitted for cyclohexyl carbons, for which specific assignments were not attempted.

Synthesis of Labelled Ru Complexes.

$RuCl_2(PCy_3)_2(=^{13}CHPh)$, *GI. In the glovebox, styrene-α-^{13}C (144 μL, 1.26 mmol, 5.0 equiv) was added to a purple solution of **GI** (208 mg, 0.253 mmol) in C_6H_6 (20 mL) in a 100 mL Schlenk tube. The reaction was stirred at RT for 45 min. The solvent was removed under vacuum to yield a purple solid, which was washed with acetone (3 x 2 mL) to remove excess styrene. The crude product (196 mg, 83% ^{13}C-enriched) was then re-subjected to styrene-α-^{13}C (146 μL, 1.28 mmol, 5.0 equiv) as before. Work-up afforded ***GI** as a dark purple powder. Yield: 177 mg (85%, 97% ^{13}C-enriched). NMR shifts are in good agreement with those reported[25] for **^{D}GI** in C_6D_6, barring those due to the alkylidene proton/deuteron. ^{13}C coupling adds complexity to the splitting patterns observed. $^{31}P\{^1H\}$ NMR (121.5 MHz, C_6D_6): δ 36.9 (d, $^2J_{PC}$ = 8.0 Hz, PCy_3). ^{1}H NMR (300.1 MHz, C_6D_6): δ 20.61 (d, $^1J_{HC}$ = 146.6 Hz, 1H, Ru=C*H*Ph), 8.72 (br s, 2H, Ph *o*-C*H*), 7.40-7.00 (m, 3H, Ph *p*-C*H*, *m*-C*H*; overlaps with solvent C_6D_5H), 2.87 (m, 6H, Cy), 2.10-1.85 (m, 12H, Cy), 1.83-1.41 (m, 30H, Cy), 1.38-1.05 (m, 18H, Cy). $^{13}C\{^1H\}$ NMR (C_6D_6, 75.5 MHz) δ 295.0 (t, $^2J_{CP}$ = 8.0 Hz, Ru), 153.4 (d, J_{CC} = 44.6 Hz, Ph *i*-*C*) 131.5 (d, J_{CC} = 2.2 Hz, Ph *o*-*C*H) 129.4 (d, J_{CC} = 4.0 Hz, Ph *m*-*C*H), 129.3 (*p*-*C*H), 32.5 (t, J_{CP} = 9.1 Hz, Cy), 30.2 (s, Cy), 28.2 (t, J_{CP} = 5.0 Hz, Cy), 27.0 (s, Cy).

$RuCl_2(PCy_3)_2(=CDPh)$, ^{D}GI: Prepared as for ***GI** above, but using styrene-α-d_1 (247 μL, 2.37 mmol, 5 equiv) and **GI** (390 mg, 0.474 mmol). Yield: 330 mg (85%, 96% ^{2}H-enriched). NMR data agree with those reported;[25] they are reproduced here for convenience. Resolution is slightly improved relative to ***GI** above. $^{31}P\{^1H\}$ NMR (121.5 MHz, C_6D_6): δ 36.7 (PCy_3). ^{1}H NMR (300.1 MHz, C_6D_6): 8.77 (d, $^3J_{HH}$ = 7.8 Hz, 2H, Ph *o*-C*H*), 7.31 (t, $^3J_{HH}$ = 7.4 Hz, 1H, Ph *p*-C*H*), 7.18-7.12 (m, 2H, Ph *m*-C*H*; overlaps with solvent C_6D_5H), 2.91 (m, 6H, Cy), 2.10-1.93 (m, 12H, Cy), 1.86-1.50 (m, 30H, Cy), 1.44-1.12 (m, 18H, Cy). ^{2}H NMR (46.1 MHz, C_6H_6): δ 20.61 ppm (br s, Ru=CD_2).

$RuCl_2(H_2IMes)(PCy_3)(=^{13}CHPh)$, *GII: In the glovebox, a 50 mL round-bottomed flask was charged with pink ***GI** (174 mg, 0.211 mmol) and THF (4.5 mL). To the stirred solution was added free H_2IMes (71 mg, 0.233 mmol, 1.1 equiv). The reaction was stirred at ambient temperature (27 °C) for 1 h, at which point an aliquot removed for ^{1}H NMR analysis revealed ca. 1% ***GI** remaining, owing to hydrolysis of H_2IMes by trace water. A further 7.0 mg H_2IMes (0.023 mmol, 0.1 equiv) was added, and stirring was continued for 30 min, at which point conversion was complete (^{1}H NMR analysis). Off-the-shelf Amberlyst 15 exchange resin (180 mg, 4.0 equiv) was added and the suspension was stirred vigorously for 1 h to sequester free PCy_3 (confirmed by ^{31}P NMR analysis). The resin was filtered off and rinsed with THF (3 x 1 mL). The filtrate was stripped to dryness to yield ***GII** as a pink powder. Yield: 155 mg (87%, 97% ^{13}C-enriched). ^{1}H NMR analysis indicated the presence of ca. 2% of the H_2IMes hydrolysis product *N,N'*-dimesityl-*N*-formylethylenediamine.[31] This impurity was removed from an 18 mg portion of the product by washing with cold pentane (3 x 1 mL): catalyst purity increased to >98%, albeit to the detriment of the isolated yield (13 mg; 72%). NMR chemical data agree well with the values reported[41] for non-labelled **GII**, with the addition of ^{13}C splitting. $^{31}P\{^1H\}$ NMR (C_6D_6): δ 30.2 (d, $^2J_{PC}$ = 8.3 Hz, PCy_3). ^{1}H NMR (300.1 MHz, C_6D_6): δ 19.64 (d, $^1J_{HC}$ = 147.9 Hz, 1H, Ru=C*H*Ph), 9.49 (br s, 1H, Ph *o*-C*H*), 7.45-5.30 (m, 8H, Ph, Mes *m*-C*H*; overlaps with solvent C_6D_5H), 3.68-0.74 (m, 55H, Cy and CH_2, CH_3 of H_2IMes). $^{13}C\{^1H\}$ NMR (C_6D_6, 75.5 MHz): δ 294.8 (d, $^2J_{CP}$ = 8.3 Hz, Ru), 221.5 (d, $^2J_{CP}$ = 77.3 Hz, C_{NHC}), 152.0 (d, $^1J_{CH}$ = 45.9 Hz, Ph *i*-*C*), 139.4 (br s), 138.3, 137.8, 137.6, 137.3 (br, s), 135.9, 130.3, 129.4, 52.2 (d, $^4J_{CP}$ = 3.3 Hz, NHC *C*H_2), 51.2 (d, $^4J_{CP}$ = 2.0 Hz, NHC *C*H_2), 32.0 (d, J_{CP} = 16.5 Hz, Cy), 29.7 (s, Cy), 28.2 (d, J_{CP} = 10.0 Hz, Cy), 26.6 (s, Cy), 21.2 (s, *p*-*C*H_3), 21.1 (s, *p*-*C*H_3), 20.5 (s, *o*-*C*H_3), 19.0 (br s, *o*-*C*H_3). Swivelling about the Ru=CHPh bond prevents observation of all phenyl carbons except the *ipso*-carbon, and broadens the corresponding ^{1}H NMR signals.

$RuCl_2(H_2IMes)(PCy_3)(=CDPh)$, ^{D}GII: Prepared as for ***GII** above, but using **^{D}GI** (275 mg, 0.334 mmol), H_2IMes (113 mg, 0.367 mmol, 1.1 equiv), and Amberlyst 15 resin (284 mg, 1.34 mmol, 4 equiv). Yield: 244 mg (86%, 96% ^{2}H-enriched). NMR chemical shifts are in excellent agreement with the values reported[41] for non-labelled **GII**, barring those due to the alkylidene proton/deuteron. ^{2}H NMR (46.1 MHz, C_6H_6): δ 19.64 ppm (br s, Ru=C*D*Ph).

$RuCl_2(PCy_3)_2(=^{13}CH_2)$, *GIm. In the glovebox, a 50 mL round-bottom flask equipped with a Kontes valve was charged with purple **GI** (403 mg, 0.490 mmol) and C_6H_6 (20 mL). The flask was removed to a Schlenk line, degassed by five consecutive freeze/pump/thaw cycles, and connected via a T-valve to the $^{13}C_2H_4$ lecture bottle and a Schlenk line. Ethylene was introduced from a lecture bottle (for details, see SI). Once a positive pressure was achieved, the reaction vessel was sealed and allowed to stir at RT. A colour change from deep purple to red, then brown, was evident within 10 min. The flask was then briefly opened to re-establish positive pressure, and resealed. The reaction was stirred for 45 min, after which the flask was returned to the glovebox and solvent was removed under vacuum. Styrene and ruthenium decomposition products were extracted with cold pentane (5 x 1.5 mL; –35 °C) to afford a pink solid consisting of ***GIm** and **GI** in 95:5 ratio (310 mg). Following a second pass of reaction with ethylene, clean ***GIm** was isolated as a pink solid. Yield 259 mg (71%, 99.5% ^{13}C-enriched). NMR data agree with those reported for **GIm**,[34] with the addition of ^{13}C splitting. $^{31}P\{^1H\}$ NMR (121.5 MHz, C_6D_6): δ 43.4 ppm (d, $^2J_{PC}$ = 8.4 Hz, PCy_3). ^{1}H NMR (300.1 MHz, C_6D_6): δ 19.41 (d, $^1J_{HC}$ = 156.7 Hz, 2H, Ru=CH_2), 2.80-2.55 (m, 6H, Cy), 2.10-1.88 (m, 12H, Cy), 1.85-1.44 (m, 30H, Cy), 1.38-1.10 (m, 18H, Cy). $^{13}C\{^1H\}$ NMR (C_6D_6, 75.5 MHz) δ

294.7 (t, $^2J_{CP}$ = 8.4 Hz, Ru=*C*H$_2$), 31.1 (t, J_{CP} = 9.6 Hz, Cy), 29.7 (s, Cy), 28.1 (t, J_{CP} = 5.3 Hz, Cy), 26.9 (s, Cy).

RuCl$_2$(PCy$_3$)$_2$(=CD$_2$), ^{D}GIm. Prepared as for ***GIm**, but using C_2D_4 and **GI** (400 mg, 0.486 mmol). Yield: 272 mg (75%, >99% ^{2}H-enriched). NMR chemical shifts are in excellent agreement with the values reported[34] for non-labelled **GIm**, barring those due to the alkylidene proton/deuteron. ^{2}H NMR (46.1 MHz, C_6H_6): δ 19.44 ppm (br s, Ru=C*D*$_2$).

RuCl$_2$(H$_2$IMes)(PCy$_3$)(=^{13}CH$_2$), *GIIm. In the glovebox, light pink ***GIm** (202 mg, 0.270 mmol) was dissolved in 12 mL C_6H_6 in a 100 mL Schlenk tube. White crystalline H_2IMes (91 mg, 0.297 mmol, 1.1 equiv) was added. The flask was removed to a Schlenk line and immersed in a 60 °C oil bath. A colour change from pink to yellow-brown was observed within 15 min, and heating was continued for a total of 45 min. The solvent was then removed under vacuum at room temperature to yield a brown residue. This brown tar was transformed into a well-behaved yellow powder by suspending in pentane in the glovebox, scratching with a spatula, and stripping off the pentane (3x). Yield 179 mg (86%) of a crude yellow solid; ^{31}P NMR analysis indicated contamination with [MePCy$_3$]Cl. Dissolving 161 mg of crude product in 8 mL benzene and washing with water (2 x 1.5 mL) removed the [MePCy$_3$]Cl impurity. The benzene was then removed under vacuum and the yellow solid was washed with cold pentane (3 x 1.5 mL) to give ***GIIm** as a fine yellow powder. Yield: 127 mg (68%, 99.5% ^{13}C-enriched). NMR chemical shifts are in excellent agreement with the values reported for the non-labelled isotopologue,[34] although ^{13}C coupling adds further complexity. ^{31}P{^{1}H} NMR (121.5 MHz, C_6D_6): δ 38.3 ppm (d, $^2J_{PC}$ = 8.5 Hz, *P*Cy$_3$). ^{1}H NMR (300.1 MHz, C_6D_6): δ 18.42 (d, $^1J_{HC}$ = 158.6 Hz, 2H, Ru=C*H*$_2$), 6.92 (s, 2H, Mes *m*-C*H*), 6.75 (s, 2H, Mes *m*-C*H*), 3.35-3.15 (m, 4H, NHC C*H*$_2$), 2.78 (s, 6H, *o*-C*H*$_3$), 2.55 (s, 6H *o*-C*H*$_3$), 2.44-2.25 (m, 3H, Cy), 2.18 (s, 3H, *p*-C*H*$_3$), 2.11 (s, 3H, *p*-C*H*$_3$), 1.70-1.45 (m, 15H, Cy), 1.30-0.95 (m, 15H, Cy). ^{13}C{^{1}H} NMR (C_6D_6, 75.5 MHz) δ 294.4 (d, $^2J_{CP}$ = 8.5 Hz, Ru=*C*H$_2$), 222.2 (d, $^2J_{CP}$ = 79.8 Hz, C_{NHC}) 139.3 (s, Mes-A *o*-*C*), 138.6 (s, Mes-A *p*-*C*), 138.1 (s, Mes-B *p*-*C*), 137.8 (s, Mes-B *o*-*C*), 137.4 (s, Mes-B *i*-*C*), 135.0 (s, Mes-A, *i*-*C*), 130.2 (s, Mes-A, *m*-*C*H), 129.7(s, Mes-B, *m*-*C*H), 51.6 (d, $^4J_{CP}$ = 3.5 Hz, NHC *C*H$_2$), 50.0 (d, $^4J_{CP}$ = 1.7 Hz, NHC *C*H$_2$), 30.7 (d, J_{CP} = 17.8 Hz, Cy), 29.2 (s, Cy), 28.0 (d, J_{CP} = 10.4 Hz, Cy), 26.7 (s, Cy), 21.22 (s, Mes *p*-*C*H$_3$), 21.20 (s, Mes *p*-*C*H$_3$), 20.1 (s, Mes-A *o*-*C*H$_3$), 19.1 (s, Mes-B *o*-*C*H$_3$). *Note*: Mes-A and Mes-B denote the two unique mesityl groups.

RuCl$_2$(H$_2$IMes)(PCy$_3$)(=CD$_2$), ^{D}GIIm. Prepared as for ***GIIm** above, but using ^{D}**GIm** (210 mg, 0.280 mmol) and free H2IMes (94 mg, 0.308 mmol). Instead of dissolving the crude product in benzene and extracting with water (an improved work-up developed with ***GIIm**), the crude product was washed with H_2O (1 x 2 mL), then washed with acetone to remove residual water (1 x 1 mL), and finally pentane (3 x 1 mL), yielding a yellow solid. Yield: 131 mg (63%, >99% ^{2}H-enriched). ^{31}P{^{1}H} and ^{1}H NMR chemical shifts are in excellent agreement with the values reported for the non-labelled isotopologue,[34] barring those due to the alkylidene proton/deuteron. ^{2}H NMR (46.1 MHz, C_6H_6): δ 18.43 ppm (br s, Ru=C*D*$_2$).

Representative procedure for C_2H_4 solubility measurements

A sample of TMB (11.2 mg, 0.066 mmol) was weighed out using an analytical balance inside the glovebox, transferred to a J. Young NMR tube, and dissolved in C_6D_6 (750 μL). The solution was degassed via five consecutive freeze/pump/thaw cycles, then opened to an atmosphere of C_2H_4 (oil-bubbler pressure) for ca. 0.5 min. The concentration of dissolved C_2H_4 was established by ^{1}H NMR analysis by comparing the integration of the C_2H_4 singlet at 5.25 ppm (4H) against the TMB aromatic singlet at 6.25 ppm (3H). A recycle delay (D_1) of 20.0 s was used to ensure accurate integration and the reported numbers are the average of three trials. The same procedure was used to measure the solubility of ethylene in CD_2Cl_2.

Representative procedure for half-life measurements

In the glovebox, a J. Young NMR tube was charged with **GIm** (10 mg, 0.013 mmol), TMB (ca. 1 mg), and THF-d_8 (0.75 mL). The initial ratio of **GIm** to TMB was measured by ^{1}H NMR analysis. The NMR probe was heated to 35 °C and ^{1}H NMR spectra were collected to 95% consumption of the starting methylidene. The half-life of **GIm** in CD_2Cl_2, $CDCl_3$, and C_6D_6 was determined similarly.

Representative procedure for amine-induced deactivation of GIIm

In the glovebox, ***GIIm** (9.8 mg, 0.013 mmol) was dissolved in C_6D_6 (633 μL) in a J Young NMR tube, and treated with H_2N^nBu (12.5 μL, 0.13 mmol; 10 equiv). The NMR tube was shaken vigorously for 10 minutes, after which ^{13}C NMR spectra were collected. Loss of the methylidene signal was accompanied by the emergence of new peaks for [*MePCy$_3$]Cl (1.5 ppm; d, $^1J_{CP}$ = 47.9 Hz) and NH^{n}Bu*Me (36.8 ppm; s), with an integration ratio of 69 : 31.

Acknowledgements

Supported by the Natural Sciences and Engineering Research Council (NSERC) of Canada.

Notes and references

[a]Center for Catalysis Research & Innovation, Chemistry Department, University of Ottawa, Ottawa, ON, Canada, K1N 6N5

Electronic Supplementary Information (ESI) available: details for handling labelled ethylene; improved synthesis of **GIIm**, and spectra for all eight complexes of Figure 1. See DOI: 10.1039/b000000x/

1. A recent book contains comprehensive updates on ring-closing metathesis (RCM) and cross-metathesis, RCM in pharma, and metathesis of renewable resources. (a) B. J. van Lierop, J. A. M. Lummiss and D. E. Fogg, in *Olefin Metathesis-Theory and Practice*, ed. K. Grela, Wiley, Weinheim, 2014, ch. 3, pp. 85-152. (b) K. Zukowska and K. Grela, in *Olefin Metathesis-Theory and Practice*, ed. K. Grela, Wiley, Weinheim, 2014, ch. 2, pp. 39-84. (c) K. R. Fandrick, J. Savoie, N. Y. Jinhua, , J. J. Song, C. H. Senanayake, ch. 12, pp. 349-366. (d) A. Nickel and R. L. Pederson, in *Olefin Metathesis-Theory and Practice*, ed. K. Grela, Wiley, Weinheim, 2014, ch. 11, pp. 335-348.
2. S. Kress and S. Blechert, *Chem. Soc. Rev.*, 2012, **41**, 4389-4408
3. U. Biermann, U. Bornscheuer, M. A. R. Meier, J. O. Metzger and H. J. Schafer, *Angew. Chem. Int. Ed.*, 2011, **50**, 3854–3871.
4. A. H. Hoveyda, S. J. Malcolmson, S. J. Meek and A. R. Zhugralin, *Angew. Chem. Int. Ed.*, 2010, **49**, 34–44.
5. G. C. Lloyd-Jones and M. P. Munoz, *J. Labelled Compd. Radiopharm.*, 2007, **50**, 1072–1087.
6. D. Schroder, *Acc. Chem. Res.*, 2012, **45**, 1521-1532.
7. C. Adlhart, C. Hinderling, H. Baumann and P. Chen, *J. Am. Chem. Soc.*, 2000, **122**, 8204–8214.
8. R. H. Grubbs, D. D. Carr, C. Hoppin and P. L. Burk, *J. Am. Chem. Soc.*, 1976, **98**, 3478–3483.
9. C. Pietraszuk, H. Fischer, S. Rogalski and B. Marciniec, *J. Organomet. Chem.*, 2005, **690**, 5912–5921.
10. R. H. Grubbs, P. L. Burk and D. D. Carr, *J. Am. Chem. Soc.*, 1975, **97**, 3265-3267.
11. C. P. Casey and H. E. Tuinstra, *J. Am. Chem. Soc.*, 1978, **100**, 2270-2272.
12. I. C. Stewart, B. K. Keitz, K. M. Kuhn, R. M. Thomas and R. H. Grubbs, *J. Am. Chem. Soc.*, 2010, **132**, 8534–8535.
13. A. Fürstner, L. Ackermann, K. Beck, H. Hori, D. Koch, K. Langemann, M. Liebl, C. Six and W. Leitner, *J. Am. Chem. Soc.*, 2001, **123**, 9000–9006.
14. J. McGinnis, T. J. Katz and S. Hurwitz, *J. Am. Chem. Soc.*, 1976, **98**, 605-606.
15. K. Tanaka, K.-I. Tanaka, H. Takeo and C. Matsumura, *J. Am. Chem. Soc.*, 1987, **109**, 2422-2425.
16. E. M. Leitao, S. R. Dubberley, W. E. Piers, Q. Wu and R. McDonald, *Chem. Eur. J.*, 2008, **14**, 11565–11572.
17. F. C. Courchay, J. C. Sworen, I. Ghiviriga, K. A. Abboud and K. B. Wagener, *Organometallics*, 2006, **25**, 6074–6086.
18. J. S. Kingsbury and A. H. Hoveyda, *J. Am. Chem. Soc.*, 2005, **127**, 4510–4517.
19. For a review describing NHC-mediated decomposition pathways, see: (a) G. C. Vougioukalakis and R. H. Grubbs, *Chem. Rev.*, 2010, **110**, 1746–1787. Theoretical studies of such intrinsic deactivation pathways have been reviewed: (b) R. Credendino, A. Poater, F. Ragone and L. Cavallo, *Catal. Sci. Technol.*, 2011, **1**, 1287-1297. Decomposition can also be mediated by unintended contaminants. Alkoxide salts are particularly aggressive, even at RT. See: (c) N. J. Beach, J. A. M. Lummiss, J. M. Bates and D. E. Fogg, *Organometallics*, 2012, **31**, 2349–2356. Alcohols in the presence of NEt_3 also promote decomposition, albeit under more forcing conditions. For leading references, see: (d) N. J. Beach, K. D. Camm and D. E. Fogg, *Organometallics*, 2010, **29**, 5450–5455, and references therein; (e) M. B. Dinger and J. C. Mol, *Organometallics*, 2003, **22**, 1089–1095; (f) S. Manzini, A. Poater, D. J. Nelson, L. Cavallo, A. M. Z. Slawin and S. P. Nolan, *Angew. Chem. Int. Ed.*, 2014, **53**, 8995-8999. In the absence of base, reaction with methanol is slow, even for **GI**: see Ref. (e). For decomposition by primary and secondary amines, see discussion below.
20. The molar receptivity of ^{13}C is 4.4 times higher than that of deuterium at comparable levels of enrichment. Furthermore, spin-spin relaxation times (T_2) for deuterium nuclei are accelerated by quadrupolar relaxation, resulting in much broader signals, as line-widths at half-height are determined by $1/\pi T_2$. See NMR properties of selected isotopes in: Bruker Almanac 2013, p. T8.
21. B. Marciniec, S. Rogalski, M. J. Potrzebowski and C. Pietraszuk, *ChemCatChem*, 2011, **3**, 904–910.
22. J. M. Bates, J. A. M. Lummiss, G. A. Bailey and D. E. Fogg, *ACS Catal.*, 2014, **4**, 2387−2394.
23. Z. Wu, S. T. Nguyen, R. H. Grubbs and J. W. Ziller, *J. Am. Chem. Soc.*, 1995, **117**, 5503–5511.
24. W. J. van Rensburg, P. J. Steynberg, W. H. Meyer, M. M. Kirk and G. S. Forman, *J. Am. Chem. Soc.*, 2004, **126**, 14332–14333.
25. M. B. Dinger and J. C. Mol, *Organometallics*, 2003, **22**, 1089–1095.
26. M. Oliván and K. G. Caulton, *J. Chem. Soc., Chem. Commun.*, 1997, 1733.
27. C. Pietraszuk and H. Fischer, *Organometallics*, 2001, **20**, 4641–4646.
28. A. Fürstner, O. R. Thiel, L. Ackermann, H.-J. Schanz and S. P. Nolan, *J. Org. Chem.*, 2000, **65**, 2204–2207.
29. A prior synthesis reported the [Ru]=CD(C_6D_5) isotopologue of ^{D}**GI**, albeit in 26% yield. See Ref. 27.
30. Workup in the Mol route involved washing with pentane (in which **GI** is more soluble) and methanol. Reaction was also carried out in dichloromethane rather than benzene. The faster rate of metathesis in aromatic media (see Ref. 28) was noted above.
31. B. J. van Lierop, A. M. Reckling, J. A. M. Lummiss and D. E. Fogg, *ChemCatChem*, 2012, **4**, 2020–2025.
32. S. H. Hong, A. G. Wenzel, T. T. Salguero, M. W. Day and R. H. Grubbs, *J. Am. Chem. Soc.*, 2007, **129**, 7961–7968.
33. M. Ulman and R. H. Grubbs, *J. Org. Chem.*, 1999, **64**, 7202–7207.
34. J. A. M. Lummiss, N. J. Beach, J. C. Smith and D. E. Fogg, *Catal. Sci. Technol.*, 2012, **2**, 1630–1632.
35. P. Schwab, R. H. Grubbs and J. W. Ziller, *J. Am. Chem. Soc.*, 1996, **118**, 100–110.
36. A single entry for benzene in the IUPAC-NIST Solubility Data Series database corresponds to the temperature and pressure regime used in our experiments, while no relevant entries exist for dichloromethane. Krauss and Gestrich reported a solubility in benzene of 140 mM at 298K, and 150 mM at 293K (see: V. W. Krauss, W. Gestrich, Khemie - Technik, 1977, **6**, 513–516). A solubility of 32 mM was reported by the Diver group in CD_2Cl_2 at room temperature and balloon pressure (see: J. A. Smulik and S. T. Diver, *J. Org. Chem.*, 2000, **65**, 1788–1792). Our study, carried out at 296 ±1.5 K and 1 atm (101.0 ±0.8 kPa), yielded values of 89 ±1 mM in C_6D_6, and 54 ±3 mM in CD_2Cl_2. To rule out potential integration errors arising from differences in the T_1 relaxation of the ethylene protons, relative to TMB, we measured the ^1H NMR spectra at different delay times. Minimal differences in relative integration (<3%) were apparent for single-pulse experiments, versus 16-scan experiments with an arbitrarily long D_1 relaxation delay.
37. M. S. Sanford, J. A. Love and R. H. Grubbs, *J. Am. Chem. Soc.*, 2001, **123**, 6543–6554.
38. Sterically accessible amines are most damaging, while α-substituted amines are relatively innocuous. For a lucid review, see: (a) P. Compain, Adv. Synth. Catal., 2007, **349,** 1829–1846. For studies of the decomposition of the Grubbs catalysts by primary amines, see (b) G. O. Wilson, K. A. Porter, H. Weissman, S. R. White, N. R. Sottos and J. S. Moore, *Adv. Synth. Catal.*, 2009, **351**, 1817–1825, and Ref. 39.
39. J. A. M. Lummiss, B. J. Ireland, J. M. Sommers and D. E. Fogg, *ChemCatChem*, 2014, **6**, 459–463.
40. A. J. Arduengo, R. Krafczyk, R. Schmutzler, H. A. Craig, J. R. Goerlich, W. J. Marshall and M. Unverzagt, *Tetrahedron*, 1999, **55**, 14523–14534.
41. L. Jafarpour, A. C. Hillier and S. P. Nolan, *Organometallics*, 2002, **21**, 442–444.

Table of Contents entry

^{13}C-Labelled Grubbs catalysts, $RuCl_2(L)(PCy_3)(=^{13}CHR)$ (R = H, Ph), pinpoint the fate of the methylidene (benzylidene) moiety during metathesis and deactivation.